

## Establishing aerosol exposure predictive models based on vibration measurements

Jhy-Charm Soo<sup>a</sup>, Perng-Jy Tsai<sup>a,b,\*</sup>, Shih-Chuan Lee<sup>a</sup>, Shih-Yi Lu<sup>c</sup>,  
Cheng-Ping Chang<sup>d</sup>, Yuh-When Liou<sup>e</sup>, Tung-Sheng Shih<sup>d,f,\*\*</sup>

<sup>a</sup> Department of Environmental and Occupational Health, Medical College, National Cheng Kung University, 138, Sheng-Li Road, Tainan 70428, Taiwan

<sup>b</sup> Sustainable Environment Research Center, National Cheng Kung University, 1 University Road, Tainan 70101, Taiwan

<sup>c</sup> School of Occupational and Health, Chung Shan Medical University, 110, Sec. 1, Jianguo N. Rd., Taichung City 40201, Taiwan

<sup>d</sup> Institute of Occupational Safety and Health, Council of Labor Affairs, Executive Yuan 99, Lane 407, Heng-ke Rd., Sijhih City, Taipei County 22143, Taiwan

<sup>e</sup> Institute of Industrial Safety and Disaster Prevention, Chia Nan University of Pharmacy & Science, 60, Erh-Jen Rd., Sec. 1, Jen-Te, Tainan 71710, Taiwan

<sup>f</sup> Graduate Institute of Environmental Health, College of Public Health, China Medical University, 91, Hsueh-Shih Road, Taichung City 40202, Taiwan

### ARTICLE INFO

#### Article history:

Received 8 November 2009

Received in revised form 14 January 2010

Accepted 14 January 2010

Available online 22 January 2010

#### Keywords:

Aerosol exposures  
Vibration measurement  
Predictive model  
Concrete drilling process

### ABSTRACT

This paper establishes particulate exposure predictive models based on vibration measurements under various concrete drilling conditions. The whole study was conducted in an exposure chamber using a full-scale mockup of concrete drilling simulator to simulate six drilling conditions. For each drilling condition, the vibration of the three orthogonal axes (i.e.,  $a_x$ ,  $a_y$ , and  $a_z$ ) was measured from the hand tool. Particulate exposure concentrations to the total suspended particulate ( $C_{TSP}$ ),  $PM_{10}$  ( $C_{PM10}$ ), and  $PM_{2.5}$  ( $C_{PM2.5}$ ) were measured at the downwind side of the drilling simulator. Empirical models for predicting  $C_{TSP}$ ,  $C_{PM10}$  and  $C_{PM2.5}$  were done based on measured  $a_x$ ,  $a_y$ , and  $a_z$  using the generalized additive model. Good agreement between measured aerosol exposures and vibrations was found with  $R^2 > 0.969$ . Our results also suggest that  $a_x$  was mainly contributed by the abrasive wear. On the other hand,  $a_y$  and  $a_z$  were mainly contributed by both the impact wear and brittle fracture wear. The approach developed from the present study has the potential to provide a cheaper and convenient method for assessing aerosol exposures from various emission sources, particularly when conducting conventional personal aerosol samplings are not possible in the field.

© 2010 Elsevier B.V. All rights reserved.

### 1. Introduction

Aerosols in working and ambient environments can pose risks to human health as they are inhaled. To date, there is strong epidemiological evidence to support the association between occupational aerosol exposures and ill-health outcomes, such as silicosis, acute silicosis, lung cancer, and chronic obstructive pulmonary disease [1–4]. For ambient environments, particulate matter (PM) pollutions are known to be detrimental to human health. For example, Pope and Dockery found the respiratory symptoms could be

related to  $PM_{10}$  pollution [5]. Schwartz and Morris found that  $PM_{10}$  pollution was associated with hospital admissions for cardiovascular diseases [6]. Several studies indicate that  $PM_{2.5}$  might have a significant effect on the increase of the mortality in adults [7–9]. Although many types of aerosol samplers have been developed for assessing PM exposures, each individual sampler was usually designed simply for collecting one specific type of particulate matter. As a result, conducting PM exposure assessment has long been subject to individual's willingness to wear aerosol samplers and the cost arising from the considerable amount of samples to be analyzed if more than one particulate exposure type is of interest at the same time [10]. Yet, it is true that some high-time resolution particle size spectrometers (e.g., Aerodynamic Particle Sizer (APS, Model 3321, TSI Inc., St. Paul, MN, USA)) can be used to directly measure particle size distributions. The resultant data can be further converted to the concentrations of the particulate of different fractions, including  $PM_{10}$  and  $PM_{2.5}$ . Because of its simplicity in measuring particle size distributions, above method has been used to characterize aerosols in different environments from various emitting sources [11–14]. But its

\* Corresponding author at: Department of Environmental and Occupational Health, Medical College, National Cheng Kung University, 138, Sheng-Li Road, Tainan 70428, Taiwan. Tel.: +886 6 2353535x5806; fax: +886 6 2752484.

\*\* Corresponding author at: Institute of Occupational Safety and Health, Council of Labor Affairs, Executive Yuan 99, Lane 407, Heng-ke Rd., Sijhih City, Taipei County 22143, Taiwan. Tel.: +886 2 26607600x551; fax: +886 2 26607730.

E-mail addresses: [pjtsa@mail.ncku.edu.tw](mailto:pjtsa@mail.ncku.edu.tw) (P.-J. Tsai), [stone@mail.ioosh.gov.tw](mailto:stone@mail.ioosh.gov.tw) (T.-S. Shih).

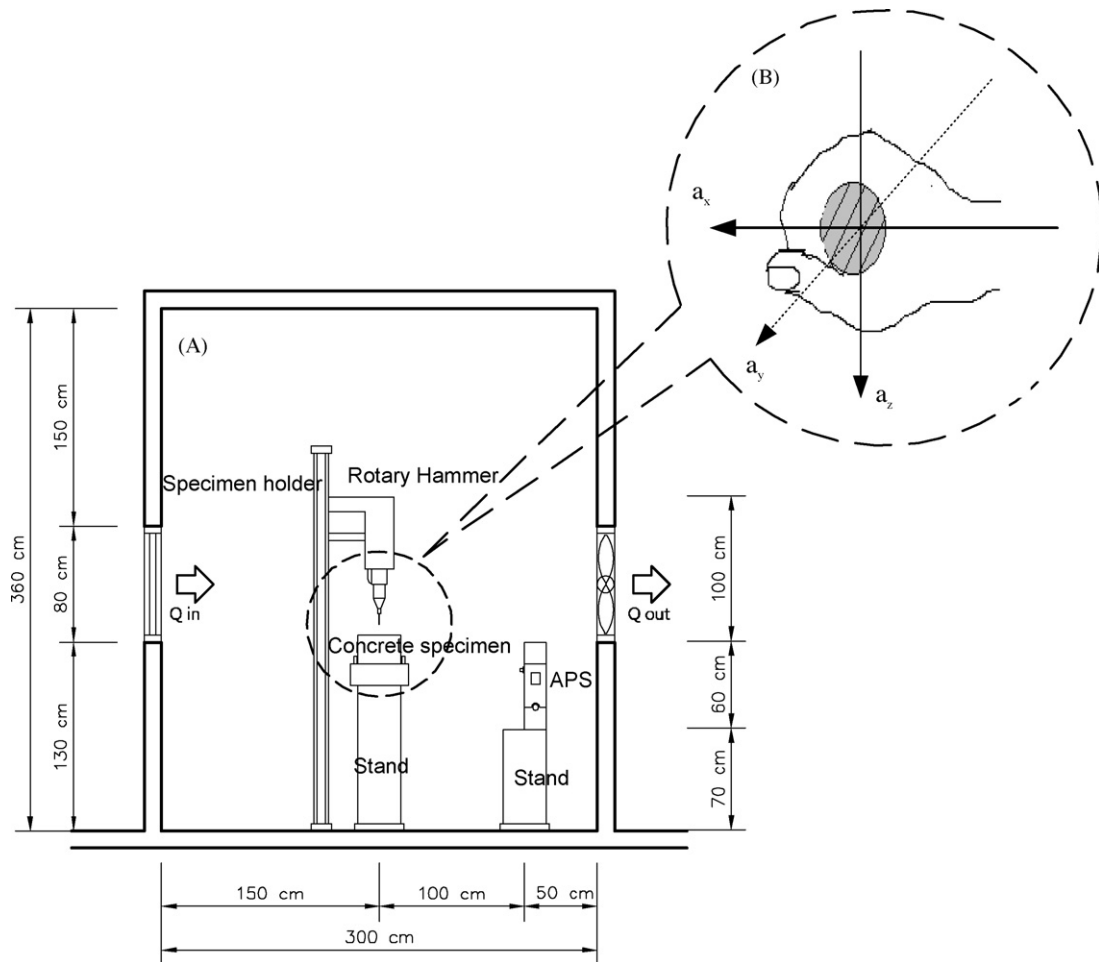


**Fig. 1.** Schematic of (A) test facilities used in the study, including a concrete drilling simulator and an APS for aerosol measurement, and (B) the X-axis, Y-axis, and Z-axis for conducting vibration measurements.

cumbersome volume and expensive cost have limited its use in the field.

In principle, the interaction between the drill bit and workpiece material is the main cause for noise, vibration and particle emissions during the drilling process [15]. Many efforts have been done to investigate vibration, noise, and aerosol exposures respectively for workers under various drilling conditions [16–22]. Moreover, the relationships between the drilling operation conditions and the characteristics of emitted particles have also been studied in several mining industries [23–26]. Vibration measurements have also been used to periodically examine the condition of the drilling tools for the maintenance purpose [16,27,28]. However, to the best of knowledge no study has been conducted to examine the relationship between the characteristics of the vibration and particles emissions.

It is known that conducting vibration monitoring is cheaper and easier than conducting conventional personal aerosol sampling in the field. Therefore, the present study was set out to examine whether the emitted vibration magnitudes could be used as a surrogate indicator to predict particulate exposures during the concrete drilling processes. The whole study was conducted in an exposure chamber using a full-scale concrete driller to simulate various drill conditions. Both vibrations and aerosol exposures were measured. Predictive models were established to relate aerosol exposures to the corresponding vibration measurement. The methodology developed from this study would be beneficial to industries for predicting particulate exposures, particularly when conducting

conventional personal aerosol sampling are not possible in the field.

## 2. Material and methods

### 2.1. Test facilities

All experimental work was performed using a full-scale mockup of concrete drilling simulator, including a rotary hammer (Hand-held Rotary Hammer, Model GBH-4 DHC, Bosch Inc., Germany), holder of machine body, specimen holder, designed for simulating the real concrete drilling process (Fig. 1) and carried out in an exposure chamber ( $L \times W \times H = 300 \text{ cm} \times 240 \text{ cm} \times 360 \text{ cm}$ ). The chamber had one air inlet ( $80 \text{ cm} \times 80 \text{ cm}$ ) and one air outlet ( $80 \text{ cm} \times 80 \text{ cm}$ ) on the opposite wall (Fig. 1). An axial fan was installed at the air outlet and inlet air was filtered. For each experiment, air velocities were measured at the cross section area designated for conducting aerosol samplings (9 points uniformly distributed in the area, see below) using a hot-wire anemometer (VelociCalc Plus, Model 8386A, TSI Inc., St. Paul, MN, USA). In the present study, the mean air velocities were consistently less than  $0.24 \text{ m s}^{-1}$  and in a good agreement with the normal indoor environment ( $<0.3 \text{ m s}^{-1}$ ) [29]. The concentration of particles inside the chamber was measured using the APS before each experiment was conducted to ensure free contamination from the previous experiment and the outside environment. The concentration of the background environment was consistently less than  $26 \text{ particles m}^{-3}$ .

## 2.2. Selected drilling operation parameters and testing conditions

Two operation parameters (and their selected testing levels), including the rotation speed ( $R_s$ : 265, 315, 460, 587 rpm) and drill bit size ( $\Phi$ : 16, 28, 32 mm) were selected in this study. The selections of the above testing levels were according to the designed range of the drilling machine and real conditions found in construction sites. All drilling conditions selected in the present study can be seen in Table 1. The concrete specimen was a 10-cm-diameter circular block and its strength (4000 psi) was the one most used in constructive operations. Four repeated drilling experiments were conducted for each selected drilling condition. For each drilling experiment, it contained nine repeated drilling runs. Each drilling run included a 30-s drilling period and followed by a 150-s rest period. As a result, the total experimental time for each drilling experiment was 27 min. For each drilling condition, we used a brand new drill bit and a new concrete specimen. The whole study was conducted using a tachometer (Hand Tachometer, Model TM 5000, Line Seiki Co. Ltd., Japan) to measure  $R_s$  for each of the nine drilling runs to examine the operation stability for each drilling experiment. We found that the resultant relative standard deviations (RSDs) for all selected  $R_s$  were consistently less than 3.90%.

## 2.3. Conducting aerosol sampling

For each selected drilling condition, aerosol samplings were conducted at the downwind side of the concrete drilling simulator (distance 100 cm) at the height of 130 cm using the APS for particle size segregating sampling to determine the concentrations of different particle size exposed to operators (Fig. 1). The sampling flow rate of the APS was  $5.0 \text{ l min}^{-1}$ . All APS measurements were conducted using the summing mode [30]. The collected data was converted to a log-normal distribution using a curve fitting program (Data Merge Software module, Model 390069, TSI Inc., St. Paul, MN, USA) assuming all collected concrete particles had a shape factor of unity and a density ( $\rho$ )  $2.30 \text{ g cm}^{-3}$  [31]. In the present study, the exposure concentration ( $C_{\text{TSP}}$ ) of the total suspended particulate (TSP) was determined by adding up the concentrations all selected particle sizes. The two exposure concentrations of the  $\text{PM}_{10}$  ( $C_{\text{PM}_{10}}$ ) and  $\text{PM}_{2.5}$  ( $C_{\text{PM}_{2.5}}$ ) were calculated based on the conventions given in the U.S. Code of Federal Regulations 40CFR53.43 and 40CFR53.62, respectively. Both the mean and RSD were presented in this study to describe the exposure concentration for each drilling condition.

## 2.4. Conducting vibration measurements

For each drilling condition, we followed the ISO 5349 [32] to determine its vibration magnitudes (expressed as a root-mean-square acceleration magnitudes,  $\text{m s}^{-2}$ ) using a human vibration meter (HVM 100, Larson Davis Inc., Depew, NY, USA). The measurements were conducted using a tri-axial PCB piezotronics with an ICP accelerometers mounded on the front handle of the rotary hammer in each of the three selected orthogonal directions (i.e., X-axis, Y-axis,

and Z-axis, as shown in Fig. 1). Above instruments (including the tri-axial ICP accelerometer) were calibrated before and after measurements using a portable vibration calibrator (calibration exciter, Type 4294, Brüel & Kjær Inc., Denmark). The energy-equivalent acceleration magnitudes for each of three orthogonal axes (i.e.,  $a_x$ ,  $a_y$ , and  $a_z$ ) were determined for each selected drilling experiment by integrating the square of the frequency-weighted acceleration magnitudes over the whole test period. The mean acceleration magnitude and its corresponding RSD were presented in this study to describe a vibration exposure.

## 2.5. Proposing predictive models

We consider that the interaction between the drilling bit and workpiece material is the main cause for vibration and particulate emissions during the drilling process. We also assume that the emitted particle size distributions could be related to the corresponding vibration magnitudes of the three orthogonal axes of  $a_x$ ,  $a_y$ , and  $a_z$ . Therefore, it can be expected that  $C_{\text{TSP}}$ ,  $C_{\text{PM}_{10}}$ , and  $C_{\text{PM}_{2.5}}$  for a given emission source are affected by its emitted vibration of the three orthogonal axes. In the present study, we adopt the generalized additive model (GAM) for the prediction purpose:

$$C_i = \alpha_i + \beta_i a_x + \gamma_i a_y + \delta_i a_z \quad (1)$$

where  $\alpha_i$  is the background concentration,  $\beta_i$ ,  $\gamma_i$ , and  $\delta_i$  are the parametric coefficients for  $a_x$ ,  $a_y$ , and  $a_z$  for the  $i$ th type of exposure concentration  $C_i$  (i.e.,  $C_{\text{TSP}}$ ,  $C_{\text{PM}_{10}}$ , or  $C_{\text{PM}_{2.5}}$ ). The use of the GAM is mainly because it has the advantage to capture the shape of the relationship between the response variable (i.e.,  $C_i$ ) and the explanatory variables (i.e.,  $a_x$ ,  $a_y$  and  $a_z$ ) by allowing non-parametric smoothers in addition to parametric forms [33]. The GAM has been widely used in many environmental health science fields for predicting ambient air pollutant concentrations and exploring the effect of air pollution on human health [34–37].

## 3. Results and discussion

### 3.1. Characteristics of aerosol exposures

Table 1 shows means and relative standard deviations (RSDs) of  $C_{\text{TSP}}$ ,  $C_{\text{PM}_{10}}$ , and  $C_{\text{PM}_{2.5}}$  for each of the six selected drilling conditions. For the drilling condition with  $\Phi$  fixed at 16 mm, we found that the increase in  $R_s$  (from 265 to 587 rpm) would result in a significant increase in  $C_{\text{TSP}}$  (from 0.083 to  $1.61 \text{ mg m}^{-3}$ ),  $C_{\text{PM}_{10}}$  (from 0.045 to  $0.498 \text{ mg m}^{-3}$ ), and  $C_{\text{PM}_{2.5}}$  (from 0.014 to  $0.042 \text{ mg m}^{-3}$ ) (trend test,  $p < 0.05$ ). For the drilling condition with the same  $\Phi$ , the increase in  $R_s$  would result in the increase in the involved drilling energy. Apparently, our results suggest that the more drilling energy was involved, the higher exposure levels could be expected.

On the other hand, the increase in  $\Phi$  would also result in more drilling energy involved in the drilling processes, if  $R_s$  remains unchanged. Therefore, it might be reasonably expected that the resultant particulate exposure levels could also be increased.

**Table 1**  
 $C_{\text{TSP}}$ ,  $C_{\text{PM}_{10}}$ , and  $C_{\text{PM}_{2.5}}$  obtained from the six selected drilling conditions.

| Drilling conditions |             | Measured exposure concentrations |         |                                |         |                                 |         |
|---------------------|-------------|----------------------------------|---------|--------------------------------|---------|---------------------------------|---------|
| $R_s$ (RPM)         | $\Phi$ (mm) | $C_{\text{TSP}}$ ( $n=4$ )       |         | $C_{\text{PM}_{10}}$ ( $n=4$ ) |         | $C_{\text{PM}_{2.5}}$ ( $n=4$ ) |         |
|                     |             | Mean ( $\text{mg m}^{-3}$ )      | RSD (%) | Mean ( $\text{mg m}^{-3}$ )    | RSD (%) | Mean ( $\text{mg m}^{-3}$ )     | RSD (%) |
| 265                 | 16          | 0.083                            | 13.8    | 0.045                          | 9.74    | 0.014                           | 2.44    |
| 315                 | 16          | 0.262                            | 14.5    | 0.099                          | 4.48    | 0.027                           | 5.46    |
| 460                 | 16          | 0.789                            | 15.3    | 0.257                          | 10.3    | 0.042                           | 9.87    |
| 587                 | 16          | 1.61                             | 12.5    | 0.450                          | 11.7    | 0.040                           | 10.6    |
| 587                 | 28          | 1.55                             | 6.39    | 0.490                          | 9.42    | 0.041                           | 14.9    |
| 587                 | 32          | 1.45                             | 11.4    | 0.530                          | 12.5    | 0.048                           | 13.5    |

Indeed, our results do reveal that, while  $R_s$  remained unchanged at 587 rpm, the increase in  $\Phi$  (from 16 to 32 mm) would result in the increase in both  $C_{PM10}$  (from 0.450 to 0.530  $\text{mg m}^{-3}$ ) and  $C_{PM2.5}$  (from 0.040 to 0.048  $\text{mg m}^{-3}$ ) (Table 1). But to the contrary, a decrease in  $C_{TSP}$  (from 1.61 to 1.45  $\text{mg m}^{-3}$ ) could also be found. Although the above trends were not statistically significant (trend test,  $p > 0.05$ ), they clearly indicate that the resultant particulate exposure levels might not be simply explained by the involved drilling energy.

It is known that the generation of particles from drilling processes involves three main mechanisms, including the impact wear, brittle fracture wear, and abrasive wear [15]. Theoretically, the first two might be related to the generation of coarse particles, and the last one could be associated with the generation of fine particles [38]. Fig. 2 shows the generated particle size distribution for the selected drilling condition with  $R_s = 587$  rpm and  $\Phi = 16$  mm for illustration. In Fig. 2A, all measured data were plotted in a log-probability scale. The resultant two distinct slopes indicate that the generated particles were in the form of bimodal. Fig. 2B shows the best fitted bimodal particle size distribution of all measured data. It contains a fine mode and a coarse mode each with a mass median aerodynamic diameter (MMAD) and geometric standard deviation ( $\sigma_g$ ) of 5.89  $\mu\text{m}$  and 1.92 and 16.01  $\mu\text{m}$  and 1.57, respectively. The above results further confirm the generated particle size distribution from the drilling process was bimodal.

Based on the results shown in Table 1, it might be reasonable to assume that the increase in  $R_s$ , if  $\Phi$  remains unchanged, would result in consistent increase in the impact wear, brittle fracture wear and abrasive wear (i.e., the increase in the generation of both coarse and fine particle fraction which leading to the increase in  $C_{TSP}$ ,  $C_{PM10}$  and  $C_{PM2.5}$ ). On the other hand, it might be also feasible to assume that the increase in  $\Phi$ , while  $R_s$  remained unchanged, might result in an increase in the abrasive wear (i.e., an increase in the generation of the fine particle fraction which leading to the increase in both  $C_{PM10}$  and  $C_{PM2.5}$ , Table 1), but decrease in both impact wear, and brittle fracture wear (i.e., an decrease in the generation of the coarse particle fraction which leading to the decrease in  $C_{TSP}$ , Table 1). Yet, it is true that the effect associated with the change of the involved drilling energy on each individual particle generation mechanism still remains unknown. However, our results clearly suggest that the magnitude of various types of dust exposure level cannot be simply explained by the magnitude of the involved drilling energy.

### 3.2. Characteristics of hand-transmitted vibration exposures

Table 2 shows the means and their corresponding RSDs of  $a_x$ ,  $a_y$ , and  $a_z$  for the six selected drilling conditions. For the drilling conditions with  $\Phi$  fixed at 16 mm, the increase in  $R_s$  (from 265 to 587 rpm) would result in a significant increase in  $a_x$  (from 0.264 to 0.658  $\text{m s}^{-2}$ ),  $a_y$  (from 0.270 to 0.678  $\text{m s}^{-2}$ ), and  $a_z$  (from 0.760 to 1.90  $\text{m s}^{-2}$ ) (trend test,  $p < 0.05$ ). Again, our results suggest that the more drilling energy (i.e., higher  $R_s$ ) involved would result

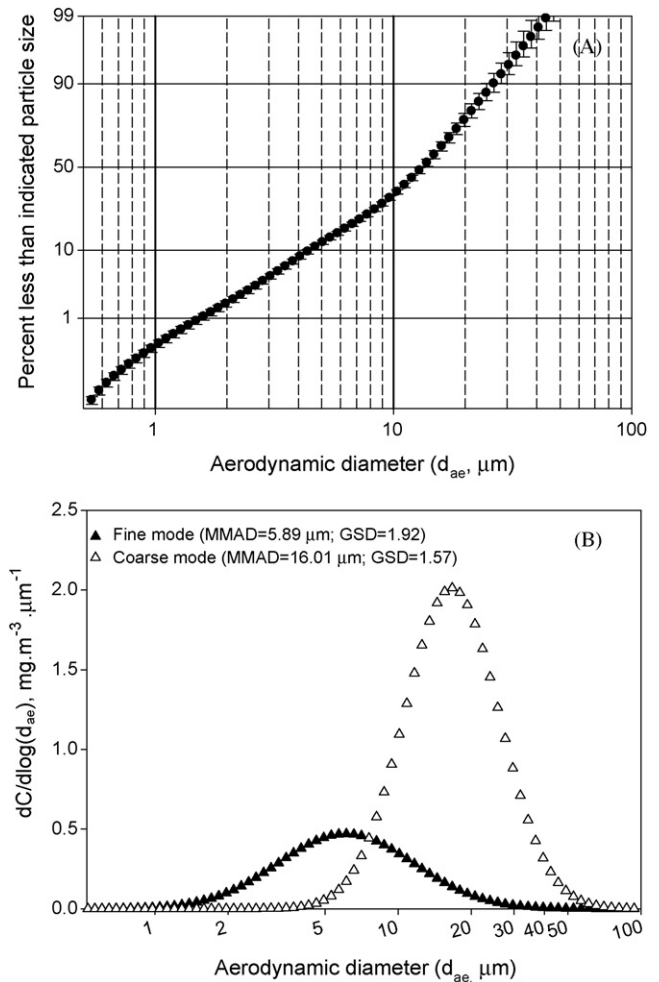


Fig. 2. The measured particle size distribution for the selected drilling condition of  $R_s = 587$  rpm and  $\Phi = 16$  mm: (A) while plotted on a log-probability plot; (B) the best fitted bimodal.

in the higher hand-transmitted vibration exposure levels. On the other hand, while  $R_s$  remained unchanged at 587 rpm, the increase in  $\Phi$  (from 16 to 32 mm) would result in the increase in vibration magnitude, including  $a_x$  (from 0.658 to 1.13  $\text{m s}^{-2}$ ),  $a_y$  (from 0.678 to 1.61  $\text{m s}^{-2}$ ), and  $a_z$  (from 1.90 to 2.62  $\text{m s}^{-2}$ ) (trend test,  $p < 0.05$ ) (see Table 2). In principle, if  $R_s$  remains unchanged for the selected drilling conditions, the increase in  $\Phi$  would result in more drilling energy involved in the drilling processes. Therefore, it can be expected that the resultant vibration magnitudes could also be increased. Yet, it is true that the three main mechanisms associated with particle emissions also affect the magnitudes of the hand-transmitted vibration [15]. Although the extent of the above effect still remains unclear, our results do suggest that the more

Table 2  
Magnitudes of  $a_x$ ,  $a_y$ , and  $a_z$  obtained from the six selected drilling conditions.

| Drilling conditions |             | Measured vibration         |         |                            |         |                            |         |
|---------------------|-------------|----------------------------|---------|----------------------------|---------|----------------------------|---------|
| $R_s$ (RPM)         | $\Phi$ (mm) | $a_x$ (n=4)                |         | $a_y$ (n=4)                |         | $a_z$ (n=4)                |         |
|                     |             | Mean ( $\text{m s}^{-2}$ ) | RSD (%) | Mean ( $\text{m s}^{-2}$ ) | RSD (%) | Mean ( $\text{m s}^{-2}$ ) | RSD (%) |
| 265                 | 16          | 0.264                      | 1.80    | 0.270                      | 1.96    | 0.760                      | 4.50    |
| 315                 | 16          | 0.350                      | 4.42    | 0.418                      | 3.45    | 1.20                       | 3.88    |
| 460                 | 16          | 0.605                      | 4.40    | 0.582                      | 1.35    | 1.59                       | 7.77    |
| 587                 | 16          | 0.658                      | 5.55    | 0.678                      | 4.66    | 1.90                       | 2.29    |
| 587                 | 28          | 0.843                      | 1.82    | 1.02                       | 4.88    | 1.98                       | 3.33    |
| 587                 | 32          | 1.13                       | 4.65    | 1.61                       | 2.40    | 2.62                       | 5.09    |



**Table 3**Regression results based on  $a_x$ ,  $a_y$ , and  $a_z$  (unit:  $\text{m s}^{-2}$ ) for predicting  $C_{\text{TSP}}$ ,  $C_{\text{PM}_{10}}$ , and  $C_{\text{PM}_{2.5}}$  (unit:  $\text{mg m}^{-3}$ ).

| Predicted exposures   | Regression coefficient |                    |                     | Intercept            | $R^2$ | MSE <sup>a</sup>      |
|-----------------------|------------------------|--------------------|---------------------|----------------------|-------|-----------------------|
|                       | $a_x$                  | $a_y$              | $a_z$               |                      |       |                       |
| $C_{\text{TSP}}$      | $0.025 \pm 0.720$      | $2.11 \pm 0.522^b$ | $0.839 \pm 0.236^b$ | $-1.27 \pm 0.148^b$  | 0.969 | 0.016                 |
| $C_{\text{PM}_{10}}$  | $-0.261 \pm 0.084$     | $0.095 \pm 0.035$  | $0.363 \pm 0.028^b$ | $-0.193 \pm 0.015^b$ | 0.999 | $2.79 \times 10^{-5}$ |
| $C_{\text{PM}_{2.5}}$ | $0.034 \pm 0.006^b$    | $0.001 \pm 0.002$  | $-0.001 \pm 0.002$  | $0.013 \pm 0.001^b$  | 0.997 | $3.10 \times 10^{-7}$ |

<sup>a</sup> The mean square error (MSE),  $\text{MSE} = \sum d^2/N$ .<sup>b</sup>  $p < 0.05$ .

drilling energy involved, the higher vibration magnitudes could be expected.

### 3.3. Predicting aerosol exposure levels based on hand-transmitted vibration measurements

Table 3 shows the resultant regression coefficients (including their standard errors and  $p$ -values) and their corresponding coefficient of determinations ( $R^2$ ) for the three proposed particulate exposure predictive models. The resultant predictive models are given as follows:

$$C_{\text{TSP}} = -1.27 + 0.025a_x + 2.11a_y + 0.839a_z \quad (R^2 = 0.969, n = 24) \quad (2)$$

$$C_{\text{PM}_{10}} = -0.193 - 0.261a_x + 0.095a_y + 0.363a_z \quad (R^2 = 0.999, n = 24) \quad (3)$$

$$C_{\text{PM}_{2.5}} = 0.013 + 0.034a_x + 0.001a_y - 0.001a_z \quad (R^2 = 0.997, n = 24) \quad (4)$$

It can be seen that the measured  $a_x$ ,  $a_y$ , and  $a_z$  can explain ~96.9, 99.9, 99.7% variations in  $C_{\text{TSP}}$ ,  $C_{\text{PM}_{10}}$ , and  $C_{\text{PM}_{2.5}}$ , respectively. Fig. 3A–C respectively compares the model predicted exposure levels (denoted as  $C_{\text{TSP}/P}$ ,  $C_{\text{PM}_{10}/P}$ , and  $C_{\text{PM}_{2.5}/P}$ , respectively) with the corresponding measured exposure levels (denoted as  $C_{\text{TSP}/M}$ ,  $C_{\text{PM}_{10}/M}$ , and  $C_{\text{PM}_{2.5}/M}$ , respectively) for the six selected drilling conditions. These figures clearly indicate that the proposed models predict quite well in both the magnitude and trend of the experimental data.

In the present study, the magnitudes of regression coefficients obtained from the three predictive models could be further used to determine the respective contributions of  $a_x$ ,  $a_y$ , and  $a_z$  to each individual type of particle exposure. We found that the magnitudes of the resultant regression coefficients presented in sequence (1) for  $a_x$  were:  $C_{\text{PM}_{2.5}} (0.034 \pm 0.006^*) > C_{\text{TSP}} (0.025 \pm 0.720) > C_{\text{PM}_{10}} (-0.261 \pm 0.084)$ ; (2) for  $a_y$  were:  $C_{\text{TSP}} (2.11 \pm 0.522^*) > C_{\text{PM}_{10}} (0.095 \pm 0.035) > C_{\text{PM}_{2.5}} (0.001 \pm 0.002)$ ; and (3) for  $a_z$  were:  $C_{\text{TSP}} (0.839 \pm 0.236^*) > C_{\text{PM}_{10}} (0.363 \pm 0.028^*) > C_{\text{PM}_{2.5}} (-0.001 \pm 0.002)$ . Here, it should be noted that only four of the above regression coefficients were statistically significant (i.e., those values with \*, including  $a_x$  in the predicting model of  $C_{\text{PM}_{2.5}}$ ;  $a_y$ , and  $a_z$  in  $C_{\text{TSP}}$ , and  $a_z$  in  $C_{\text{PM}_{10}}$ ). Based on the above results, it can be concluded that the increase in  $a_x$  would result in the increase in the particle exposure concentration with high fine particle fraction (i.e.,  $C_{\text{PM}_{2.5}}$ ). On the other hand, the increase in both  $a_y$  and  $a_z$  would consistently result in the increase of those with high coarse particle fraction (i.e.,  $C_{\text{TSP}}$  and  $C_{\text{PM}_{10}}$ ). It is known that the generation of coarse particles was mainly contributed by the two mechanisms of the impact wear and brittle fracture wear, and the generation of fine particles was mainly by the mechanism of the abrasive wear [38]. Based on the results obtained from this study and the above inference, it would be reasonable to expect that  $a_x$  might be mainly contributed by the abrasive wear. On the other hand,  $a_y$  and  $a_z$  could be mainly by both the impact wear and brittle fracture wear.

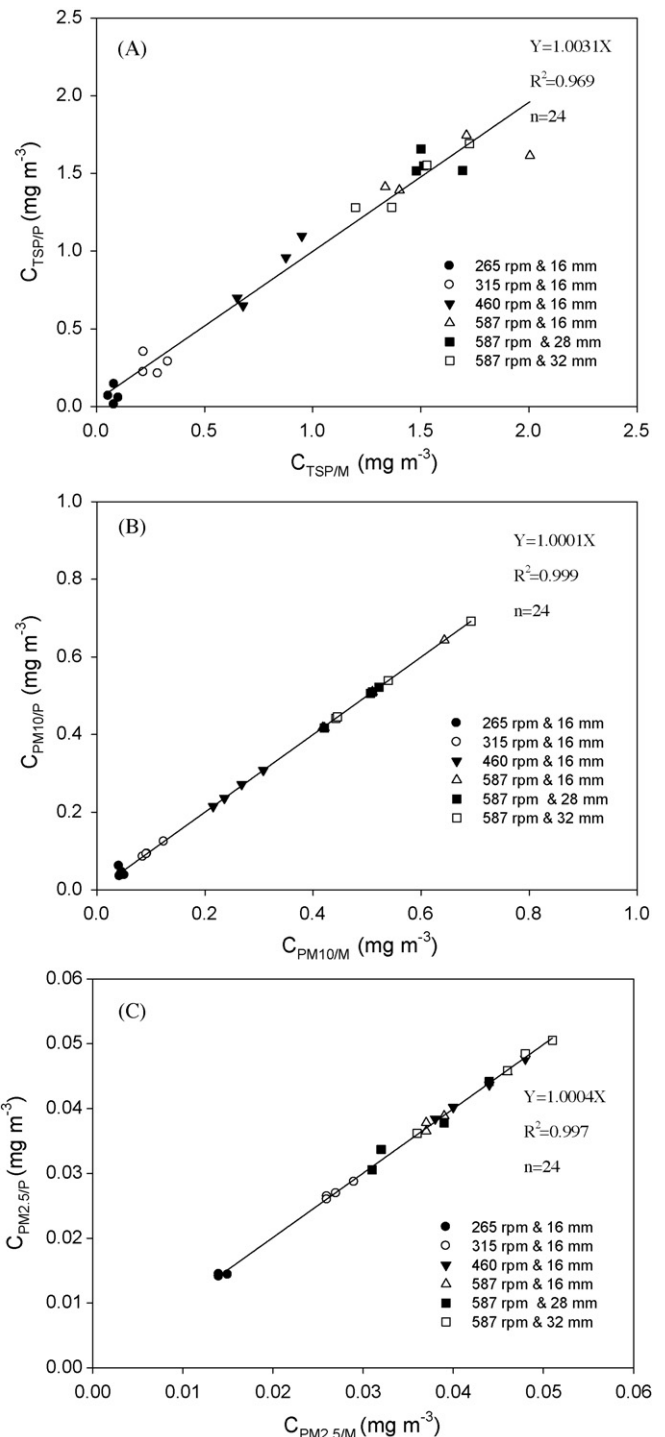


**Fig. 3.** Comparison the predicted concentrations with measured concentrations: (A)  $C_{\text{TSP}/P}$  vs.  $C_{\text{TSP}/M}$ ; (B)  $C_{\text{PM}_{10}/P}$  vs.  $C_{\text{PM}_{10}/M}$ ; (C)  $C_{\text{PM}_{2.5}/P}$  vs.  $C_{\text{PM}_{2.5}/M}$ .

#### 4. Conclusions

In this study, we found that the magnitude of various types of dust exposure level cannot be simply explained by the magnitude of the involved drilling energy. But for the hand-transmitted vibration, we found that the more drilling energy involved, the higher vibration magnitudes could be expected. Empirical models for predicting  $C_{TSP}$ ,  $C_{PM10}$  and  $C_{PM2.5}$  were done based on measured  $a_x$ ,  $a_y$ , and  $a_z$  using the generalized additive model. Good agreement between measured aerosol exposures and vibrations was found with  $R^2 > 0.969$ . It can be concluded that the increase in  $a_x$  would result in the increase in  $C_{PM2.5}$ . On the other hand, the increase in both  $a_y$  and  $a_z$  would consistently result in the increase in both  $C_{TSP}$  and  $C_{PM10}$ . In addition, our results also suggest that  $a_x$  was mainly contributed by the abrasive wear. On the other hand,  $a_y$  and  $a_z$  were dominantly contributed by both the impact wear and brittle fracture wear. The approach developed from the present study have the potential to provide a cheaper and convenient method for assessing aerosol exposures from various emission sources, particularly for those conducting conventional personal aerosol samplings are not possible in the field.

#### Acknowledgement

The authors wish to thank the Institute of Occupational Safety and Health (IOSH) of the Council of Labor Affairs of Taiwan for funding this research project.

#### References

- [1] N.M. Cherry, G.L. Burgess, S. Turner, J.C. McDonald, Crystalline silica and risk of lung cancer in the potteries, *Occup. Environ. Med.* 55 (1998) 779–785.
- [2] K. Steenland, A. Mannetje, P. Boffetta, L. Stayner, M. Attfield, J. Chen, M. Dosemeci, N. Deklerk, E. Hnizdo, R. Koskela, H. Checkoway, Pooled exposure–response analysis and risk assessment for lung cancer in 10 cohorts of silica-exposed workers: an IARC multicentre study, *Cancer Causes Control* 12 (2001) 773–784.
- [3] J.M. Hughes, H. Weill, R.J. Rando, R. Shi, A.D. McDonald, J.C. McDonald, Cohort mortality study of North America industrial sand workers. II. Case-referent analysis of lung cancer and silicosis death, *Ann. Occup. Hyg.* 45 (2001) 201–207.
- [4] J.C. McDonald, A.D. McDonald, J.M. Hughes, R.J. Rando, H. Weill, Mortality from lung and kidney disease in a cohort of North American industrial sand workers: an update, *Ann. Occup. Hyg.* 49 (2005) 367–373.
- [5] C.A. Pope III, D.W. Dockery, Acute health effects of  $PM_{10}$  pollution in Utah Valley, *Arch. Environ. Health* 47 (1992) 211–217.
- [6] J. Schwartz, R. Morris, Air pollution and hospital admissions for cardiovascular disease in Detroit, MI, *Am. J. Epidemiol.* 142 (1995) 927–939.
- [7] D.W. Dockery, C.A. Pope III, X. Xu, J.D. Spengler, J.H. Ware, M.E. Fay, B.G. Ferris Jr., F.E. Speizer, An association between air pollution and mortality in six U.S. cities, *N. Engl. J. Med.* 329 (1993) 1753–1759.
- [8] C.A. Pope III, M.J. Thun, M.M. Namboodiri, D.W. Dockery, J.S. Evans, F.E. Speizer, C.W. Heath Jr., Particulate air pollution is a predictor of mortality in a prospective study of U.S. adults, *Am. J. Respir. Crit. Care Med.* 151 (1995) 669–674.
- [9] J. Schwartz, D.W. Dockery, L.M. Neas, Is daily mortality associated significantly with fine particles, *J. Air Waste Manage. Assoc.* 46 (1996) 927–939.
- [10] T.J. Buckley, J.M. Waldman, N.C.G. Freeman, P.J. Liroy, V.A. Marple, W.A. Turner, Calibration, intersampler comparison, and field application of a new  $PM_{10}$  personal air-sampling impactor, *Aerosol Sci. Technol.* 14 (1991) 380–387.
- [11] S. Shen, P.A. Jaques, Y. Zhu, M.D. Geller, C. Sioutas, Evaluation of the SMPS-APS system as a continuous monitor for measuring  $PM_{2.5}$ ,  $PM_{10}$  and coarse ( $PM_{2.5-10}$ ) concentrations, *Atmos. Environ.* 36 (2002) 3939–3950.
- [12] J.D. Yanosky, P.L. Williams, D.L. MacIntosh, A comparison of two direct-reading aerosol monitors with the federal reference method for  $PM_{2.5}$  in indoor air, *Atmos. Environ.* 36 (2002) 107–113.
- [13] J. Pagels, M. Strand, J. Rissler, A. Szpila, A. Gudmundsson, M. Bohgard, L. Lillieblad, M. Sanati, E. Swietlicki, Characteristics of aerosol particles formed during grate combustion of moist forest residue, *J. Aerosol Sci.* 34 (2003) 1043–1059.
- [14] T. Ferge, J. Maguhn, H. Felber, R. Zimmermann, Particle collection efficiency and particle re-entrainment of an electrostatic precipitator in a sewage sludge incineration plant, *Environ. Sci. Technol.* 38 (2004) 1545–1553.
- [15] E. Rabinowicz, *Friction and Wear of Materials*, 2nd ed., John Wiley and Son, Inc., New York, 1995.
- [16] S.E. Keith, A.J. Brammer, Rock drill handle vibration—measurement and hazard estimation, *J. Sound Vibr.* 174 (1994) 475–491.
- [17] T.I. El-Wardany, D. Gao, M.A. Elbestawi, Tool condition monitoring in drilling using vibration signature analysis, *Int. J. Mach. Tools Manuf.* 36 (1996) 687–711.
- [18] P.V. Bayly, M.T. Lamar, S.G. Calvert, Low-frequency regenerative vibration and the formation of lobed holes in drilling, *J. Manuf. Sci. Eng.-Trans. ASME* 124 (2002) 275–285.
- [19] D.J. Edwards, G.D. Holt, Exposure to hand-arm vibration: implications of new statutory requirements, *Build. Res. Inform.* 33 (2005) 257–266.
- [20] J.I. Phillips, P.S. Heyns, G. Nelson, Rock drills used in South African mines: a comparative study of noise and vibration levels, *Ann. Occup. Hyg.* 51 (2007) 305–310.
- [21] A.N. Rimell, L. Notini, N.J. Mansfield, D.J. Edwards, Variation between manufacturers' declared vibration emission values and those measured under simulated workplace conditions for a range of hand-held power tools typically found in the construction industry, *Int. J. Ind. Ergon.* 38 (2008) 661–675.
- [22] D.K. Verma, A. Sebestyen, J.A. Julian, D.C.F. Muir, D.S. Shaw, R. Macdougall, Particle-size distribution of an aerosol and its subfraction, *Ann. Occup. Hyg.* 38 (1994) 45–58.
- [23] H.W. Shen, H.R. Hardy, A.W. Khair, Laboratory study of acoustic emission and particle size distribution during rotary cutting, *Int. J. Rock Mech. Min. Sci. Geomech. Abstr.* 34 (1997) 635–636.
- [24] V.B. Achanti, A.W. Khair, Bit geometry effects on failure characteristics of rock, *Min. Eng.* 52 (2000) 101–107.
- [25] V.B. Achanti, A.W. Khair, Cutting efficiency through optimised bit configuration—an experimental study using a simulated continuous miner, *Miner. Resour. Eng.* 10 (2001) 427–434.
- [26] S.J. Page, R. Reed, J.M. Listak, An expanded model for predicting surface coal mine drill respirable dust emissions, *Int. J. Min. Reclam. Environ.* 22 (2008) 210–221.
- [27] E. Jantunen, A summary of methods applied to tool condition monitoring in drilling, *Int. J. Mach. Tools Manuf.* 42 (2002) 997–1010.
- [28] S. Braun, E. Lenz, C.L. Wu, Signature analysis applied to drilling, *J. Manuf. Sci. Eng.-Trans. ASME* 104 (1982) 268–276.
- [29] P.E.J. Baldwin, A.D. Maynard, A survey of wind speeds in indoor workplaces, *Ann. Occup. Hyg.* 42 (1998) 303–313.
- [30] T.M. Peters, D. Leith, Concentration measurement and counting efficiency of the aerodynamic particle sizer 3321, *J. Aerosol Sci.* 34 (2003) 627–634.
- [31] J.F.Y. Sidney Mindess, *Concrete*, Prentice-Hall, Englewood Cliffs, NJ, 1981.
- [32] International Organization for Standardization (ISO), *Mechanical Vibration—Guidelines for the Measurement and the Assessment of Human Exposure to Hand-transmitted Vibration*, ISO 5349, ISO, Geneva, 1986.
- [33] T.J. Hastie, R.J. Tibshirani, *Generalized Additive Models*, Chapman and Hall, New York, 1990.
- [34] S.N. Wood, N.H. Augustin, GAMs with integrated model selection using penalized regression splines and applications to environmental modeling, *Ecol. Model.* 157 (2002) 157–177.
- [35] J.M. Davis, P. Speckman, A model for predicting maximum and 8 h average ozone in Houston, *Atmos. Environ.* 33 (1999) 2487–2500.
- [36] A.L.F. Braga, A. Zanobetti, J. Schwartz, The effect of weather on respiratory and cardiovascular deaths in 12 US cities, *Environ. Health Perspect.* 110 (2002) 859–863.
- [37] Y. Liu, C.J. Paciorek, P. Koutrakis, Estimating regional spatial and temporal variability of  $PM_{2.5}$  concentrations using satellite data, meteorology, and land use information, *Environ. Health Perspect.* 117 (2009) 886–892.
- [38] J.C. Soo, P.J. Tsai, C.H. Chen, D.J. Hsu, Y.T. Dai, C.P. Chang, Establishing aerosol exposure predictive models based on noise measurements—using concrete drilling as an example, *J. Environ. Monit.* 11 (2009) 1523–1528.